Depth of focus and visual acuity with primary and secondary spherical aberration

Fan Yi[1], D. Robert Iskander[2], Michael Collins[1]

Contact Lens and Visual Optics Laboratory, School of Optometry, Queensland University of Technology, Brisbane, Australia

[2]Institute of Biomedical Engineering and Instrumentation, Wroclaw University of Technology, Wroclaw, Poland

ABSTRACT

It is known that the depth of focus (DOF) of the human eye can be affected by the higher order aberrations. We estimated the optimal combinations of primary and secondary Zernike spherical aberration to expand the DOF and evaluated their efficiency in real eyes using an adaptive optics system. The ratio between increased DOF and loss of visual acuity was used as the performance indicator. The results indicate that primary or secondary spherical aberration alone shows similar effectiveness in extending the DOF. However, combinations of primary and secondary spherical aberration with different signs provide better efficiency for expanding the DOF. This finding suggests that the optimal combinations of primary and secondary spherical aberration may be useful in the design of optical presbyopic corrections.

Keywords: depth of focus, higher order aberrations, retinal image quality metric, adaptive optics.

1. Introduction

The depth of focus (DOF) of the human eye serves a mechanism of blur tolerance. As long as the target image remains within the DOF in the image space, the eye will still perceive the image as being clear. A large DOF is especially important for presbyopic patients with partial or complete loss of accommodation, since this helps them to obtain an acceptable retinal image when viewing a target moving through a range of near to intermediate distances.

The DOF of the human eye can be affected by a variety of optical and neural factors (Wang & Ciuffreda, 2006). Higher order aberrations (HOA) are one of the important optical factors that influence DOF. Nio et al. (2002) found that HOA helps to increase the DOF, while at the same time lowering the modulation transfer at higher frequencies. Recently, Rocha et al. (2009) investigated the different effect of individual 3rd and 4th order Zernike polynomial coefficients (spherical aberration, coma and trefoil) on DOF using an adaptive optics (AO) system. It was found that certain amounts of spherical aberration can significantly enhance the DOF, while other HOAs only had minimal effect on DOF. Using adaptive optics, Benard et al (2010) also reported an increased DOF with primary spherical aberration (Z_4^0) and further enhanced DOF with some combinations of primary (Z_4^0) and secondary (Z_6^0) spherical aberration.

The structure of HOA in the human eye is not static. Studies of wavefront aberrations during accommodation have revealed significant changes in HOA of young eyes under different accommodation levels (Atchison et al., 1995; He et al., 2000; Ninimiya et al., 2002; Cheng et al., 2004a). These changes dynamically alter the structure of HOA of the eye and affect most noticeably the Zernike coefficient terms of primary, Z_4^0, spherical aberration (Ninomiya et al., 2002; Cheng et al., 2004a;). Ninomiya et al. (2002) compared the monochromatic wavefront aberrations of young adults measured with far viewing (0 D) and at a 3.0 D accommodative level. They found significant changes of both Z_4^0 and Z_6^0 during accommodation. In the study of Cheng et al. (2004a), the wavefront aberrations in a large young adult population were studied for accommodative stimuli up to 6.0 D. The authors reported a significant negative shift of Z_4^0 as the accommodative level increased, while the Z_6^0 showed a trend (not significant) towards more positive values. Similar findings were also reported by Lopéz-Gil and Fernández-Sánchez (2010), who performed theoretical and ray-tracing calculations on an accommodative eye model, and wavefront measurements in real eyes. A decrease of primary, Z_4^0, and an increase of secondary, Z_6^0, spherical aberration were found in both conditions.

In this study, we aimed to investigate the effect of primary spherical aberration, secondary spherical aberration and their various combinations on DOF and visual acuity by using an adaptive optics system. The effects of Z_4^0, Z_6^0 and their combinations on the DOF of a simulated diffraction-limited model eye were investigated using a through-focus simulation algorithm, and optimal combinations of Z_4^0 and Z_6^0 were estimated. Then, the effect of those combinations of Z_4^0 and Z_6^0 on the DOF and visual acuity of real eyes was investigated through the use of an AO system.

2. Methods

2.1 Extending the DOF in a simulated model eye

To understand the effect of primary and secondary spherical aberration on the through-focus performance of the eye and to estimate a set of optimal combinations for extending the DOF in an experiment with the AO system described later, we first studied the DOF in an unaberrated diffraction-limited eye model.

A dedicated simulation program was written from first principles in MATLAB (The MathWorks, Inc., Natick, MA) to theoretically apply a number of possible combinations of Z_4^0 and Z_6^0 to a model eye and to calculate the DOF based on an image quality metric (IQM). The algorithm of the through-focus calculation (Steps 1 to 7) was presented in detail in our earlier study (Yi, Iskander & Collins, 2010). Here the algorithm is extended to include secondary spherical aberration.

The flow chart of the simulation program is shown in Figure 1a and an example of the simulation output is shown in Figure 1b. A set of Zernike polynomials from the wavefront data of one myopic subject was used here as an example to illustrate the output of the through-focus simulation. The pupil diameter used for analysis was 5 mm and the total HOA RMS of the subject was 0.28 µm. The major higher order aberration components of the original wavefront include -0.14 µm of vertical trefoil (Z_3^{-3}), 0.19 um of vertical coma (Z_3^{-1}), 0.05 µm of horizontal coma (Z_3^{1}) and 0.08 µm of tetrafoil at zero degree (Z_4^{4}). The modified through-focus VSOTF curve was obtained after an arbitrary level of 0.3 µm of primary spherical aberration (Z_4^{0}) was added to the subject's original wavefront pattern. The introduction of different levels of Z_4^0 and Z_6^0 may change the characteristics of the subject's though-focus IQM and therefore affect the predicted DOF. A shift of centre of focus (COF) could also occur due to the interaction of defocus and the induced HOA.

2.1.1 Through-focus algorithm to calculate the DOF of a simulated model eye

In the algorithm, DOF is theoretically defined as the range of defocus error which degrades the retinal image quality to a certain level of the maximum possible value. We chose the visual Strehl ratio based on the optical transfer function (VSOTF) to estimate the retinal image quality, since it is currently considered as one of the best descriptors of visual performance that can be directly derived from wavefront aberrations (Marsack et al., 2004). It was also reported as a retinal image quality metric that correlated well with the through-focus visual acuity (VA) defined in logMAR in healthy eyes (Cheng et al., 2004b). We use the augmented version of VSOTF (Iskander, 2006) defined as

$$VSOTF = \frac{\int_{-\infty}^{\infty}\int_{-\infty}^{\infty} CSF_N(f_x, f_y)\cdot\left|\mathrm{Re}\left(OTF(f_x, f_y)\right)\right| df_x df_y}{\int_{-\infty}^{\infty}\int_{-\infty}^{\infty} CSF_N(f_x, f_y)\cdot OTF_{DL}(f_x, f_y)\, df_x df_y} \quad (1)$$

where $OTF_{DL}(f_x, f_y)$ denotes the diffraction limited optical transfer function, $CSF_N(f_x, f_y)$ is the neural contrast sensitivity function, and (f_x, f_y) are the spatial frequency coordinates. Here the VSOTF was based on calculated optical transfer function across all spatial frequencies up to 60 cycles per degree (Iskander, 2006).

(Insert Figure 1 here)

2.1.2 Image quality threshold

It is important for the human eye to maintain an acceptable level of retinal image quality after any potential extension of DOF. However, in a linear optical system, the extension of DOF always comes at the price of lower image quality producing a compromise between image quality (calculated by an IQM such as VSOTF, for example) and the potential increase in DOF.

In an earlier study conducted by Plakitsi and Charman (1995), the authors chose a visual acuity (VA) level of 0.3 logMAR to define the DOF, which was treated as an adequate standard of distant vision for driving. For daily activities, involving near work and visually intensive tasks such as reading, a modest level of VA loss will also lead to significant loss of performance. In a study of visual acuity and contrast sensitivity including 2520 older subjects, West et al (2002) found that about 50% of the studied population with visual acuity worse than 0.2 logMAR had a difficulty of reading. Using a method similar to Plakitsi and Charman (1995), Collins and coauthors (2002) adopted the level of 0.2 logMAR VA to measure the "absolute" DOF for a group of young adult subjects wearing contact lenses (with various levels of spherical aberration). The "absolute" DOF was defined as the range of defocus over which the VA is within the 0.2 logMAR of the subject's best possible acuity. Therefore an absolute VA level of 0.2 logMAR was adopted as a preset image quality threshold, which should be maintained as DOF of the eye is extended. In the through-focus algorithm, the 0.2 logMAR level corresponds to VSOTF of approximately 0.12 (see Figure 1b) based on estimates from the results obtained by Cheng, Bradley and Thibos (2004). The theoretical DOF can be then estimated as the range of defocus error (positive and negative) that degrades the through-focus VSOTF value to 0.12 under the influence of various combinations of Z_4^0 and Z_6^0. While the 0.2 logMAR (VSOTF = 0.12) criterion has been adopted for all through-focus simulations in this study, the same methods can be used for any chosen value of logMAR or VSOTF.

2.1.3 Estimation of the optimal levels of Z_4^0 and Z_6^0 combination

The influence of different levels of Z_4^0 and Z_6^0 on the theoretical DOF of the diffraction-limited model eye with a 6 mm pupil is shown in Figure 2, derived from the through-focus algorithm illustrated in Figure 1a. The range of simulation was set based on the HOA RMS which can be stably generated by the Mirao52 deformable mirror (Sabesan et al, 2007), which include Z_4^0 ranged from –0.8 μm to 0.8 μm in 0.1 μm steps (17 levels), and the Z_6^0, ranged from –0.25 μm to 0.25 μm in 0.05 μm steps (11 levels). ΔDOF is defined as the difference between the DOF achieved for a particular non-zero combination of Z_4^0 and Z_6^0 and the DOF for $Z_4^0 = 0$ and $Z_6^0 = 0$. Higher levels of spherical aberration than those shown in Figure 2 were not considered, since they decreased the image quality metric below the defined level of 0.2 logMAR (VSOTF < 0.12). Figure 2a shows the response of ΔDOF as a function of different combinations of Z_4^0 and Z_6^0 (a total of 187 combinations). The area with a lighter shade of grey indicated the wavefront combination providing a larger increase of DOF of the model eye. Figures 2b and 2c show the two dimensional "slices" from Figure 2a and represent the ΔDOF at zero-Z_6^0 and zero-Z_4^0 levels, respectively.

The maximum VSOTF value only occurs when Z_4^0 and Z_6^0 are both zero. It is evident that combinations of Z_4^0 and Z_6^0 with opposite sign can significantly extend the DOF of the model eye, within the constraints of not reducing VSOTF below 0.12 (i.e., equivalent to 0.2 logMAR loss). On the other hand, introducing Z_4^0 and Z_6^0 of the same sign is not as effective at extending DOF. For example, if we take 0.2 microns of Z_4^0 and Z_6^0 with opposite signs, we find a predicted increase of DOF of 2.2 D (Figure 2a). Whereas if we take 0.2 microns of Z_4^0 and Z_6^0 with the same sign, we find a predicted increase of DOF of 1.5 D (Figure 2a).

To further reduce the number of possible combinations of Z_4^0 and Z_6^0, from the total of 17 × 11 = 187, a radial sampling procedure of the ΔDOF matrix (Figure 2a) starting from the point of $Z_4^0 = 0$ and $Z_6^0 = 0$ was performed to determine the wavefront combinations which theoretically provide largest extension of DOF at different combined wavefront RMS levels, defined by:

$$RMS_{Total} = \sqrt{(RMS_{Z40})^2 + (RMS_{Z60})^2}.$$

Eighteen such wavefront combination of Z_4^0 and Z_6^0 were obtained from the radial sampling procedure. Thirteen levels of pure Z_4^0 ranging from -0.6 to +0.6µm with a step of 0.1µm, and 10 levels of pure Z_6^0 ranging from -0.25 to +0.25µm with a step of 0.05µm were also included. This procedure reduced the number of candidate combinations to 41, which are indicated in Figure 2a by the overlaid box shape.

(Insert Figure 2 here)

2.2 Measurement of DOF in real eyes

After investigating the effect of different combinations of Z_4^0 and Z_6^0 on DOF with a diffraction limited model eye, these 41 pre-determined wavefront combinations of Z_4^0 and Z_6^0 were then applied to a group of human eyes using an adaptive optics system and the effect on DOF was measured.

2.2.1 Subjects

Six students (3 males and 3 females) from the School of Optometry, Queensland University of Technology participated in this study. The mean age of the subjects was 29, ranging from 26 to 33 years. The group had a mean spherical equivalent refractive error of –1.0 ±2.0 D, (ranging from –5.0 to 0 D) and a mean astigmatism of –0.21 ±0.25 D (ranging from –0.5 to 0 D) in the tested eyes. All subjects had good ocular health with best-corrected Snellen visual acuity of at least 6/6 in the tested eye. The value of higher order ocular aberrations were measured with a Complete Ophthalmic Analysis System (COAS, Wavefront Science Inc.) from the left eye of the six subjects and analyzed for a 6 mm pupil diameter. For each subject, a series of 4 x 30 dynamic wavefront measurements were acquired at the sampling rate of about 10 Hz. The average wavefront aberration was then calculated for each of the subjects. Analysis of the wavefront aberrations was conducted up to the 6th radial order using two radial orders lower than the original wavefront fit (Neal et al., 2005). The RMS of total HOA from the six eyes was 0.37 ±0.10 μm for a 6 mm pupil. The mean value of Z_4^0 was 0.13 ±0.09 μm, which was more than 10 times larger than the mean value of Z_6^0 at 0.01 ±0.01 μm. These values for total HOA and Z_4^0 are within the normal ranges of value reported by Porter et al (2001) and Wang and Koch (2003).

The study followed the requirements of the university human research ethics committee and was conducted in accordance with the tenets of the Declaration of Helsinki. Informed consent was obtained from all subjects who participated in the study.

2.2.2 Apparatus

A customized AO system was constructed for the experiment. The AO system was capable of measuring and changing the wavefront aberration of the eye and of measuring the DOF under the influence of different combinations of HOA. The system was based on two major components: the HASO32^{TM} Hartmann Shack wavefront sensor and the Mirao52™ deformable mirror (both from Imagine Eyes, Orsay, France). In a pilot study, the HASO32™ wavefront sensor was first calibrated with a model eye with known levels of aberration and then benchmarked against a Complete Ophthalmic Analysis System (COAS™, Wavefront Science, Inc) with 10 cyclopleged human eyes. The results between sensors showed reasonable correlation and good repeatability. Performance of the Mirao52™ deformable mirror to generate single wavefront modes up to the 5th and 6th Zernike radial order was earlier evaluated by Fernández et al (2006) and Sabesan et al (2007). In a pilot study, the mirror's capability of generating combinations of primary and secondary spherical aberration was investigated. Within the calibration range (Z_4^0 =-0.8 to 0.8 μm, Z_6^0=-0.25 to 0.25 μm), good correlation was observed between the predicted and generated wavefront ($R_{Z(4,0)}$ =0.97 and $R_{Z(6,0)}$=0.98) and the generation of Z_4^0 and Z_6^0 was found to be independent to each other. However, limited by actuator stroke, more wavefront combinations can be generated when Z_4^0 and Z_6^0 coefficients have different signs rather than when they have the same sign.

(Insert Figure 3 here)

The optical layout of the AO system conjugates the exit pupil plane of the subject with the surface of deformable mirror and the Hartmann Shack wavefront sensor (Figure 3). A 10-D achromatic lens L1 is placed in front of the eye, with its back focal point located at the eye's entrance pupil. Two pairs of relay lenses L5 and L4 as well as L3 and L2 are set up in an afocal form. Through the two sets of lenses the fixation target forms an image at the back focal point of L2, which acts as the object of Badal lens L1 and its distance to L1 is controlled by the movement of the Badal stage. In this configuration, every 1 cm movement of the object brings approximately 1 D of change in the target vergence. The fixation target consists of a logMAR letter chart printed on a sheet of clear plastic. Two different letter charts were used to measure the subject's visual acuity to reduce learning effects. A distant white LED light source was used to back illuminate the target through a diffuser. The target's contrast was 80% with an overall luminance of 120 cd/m^2. The letter size on the chart was scaled to provide a range of visual angles from 20 min of arc (0.6 logMAR detail, the top line of chart) to 2.5 min of arc (–0.3 logMAR detail, the bottom line of chart) when viewed through the AO system optics.

The position of the subject's pupil was continuously monitored and controlled. The CASAO control software (Imagine Eyes, Orsay, France) was used to check and realign the subject's pupil position at the beginning and the end of each measurement section when a different wavefront combination was induced. A customized heavy head rest was used to position the subject's head. Its position with respect to the wavefront sensing system could be adjusted when a displacement of larger than 0.3 mm was observed.

2.2.3 Protocol

All subjects were experienced with visual psychophysics experiments requiring viewing of targets through a Badal optical system. To allow the subjects to become familiar with the task of recognizing the "objectionable blur" level (Atchison et al., 2005), each of them was given a short training on the AO system with different levels of induced defocus. Following this, the subject's tested eye was cyclopleged and dilated by 2 drops of cyclopentolate (1% Minims, 0.5 ml, Bausch & Lomb Australia). The measurements started about 30 minutes later after the full effect of cycloplegia was reached (Manny et al., 1993).

Under full cycloplegia and pupillary dilation, the subject was instructed to fixate on the 0.2 logMAR line on the displayed Bailey-Lovie letter chart through a 6 mm artificial pupil, with the fellow eye occluded by a black eye patch. The subject's defocus level was controlled by moving the Badal stage and the astigmatism derived from the individual subjective refraction was corrected using a trial lens mounted in front of the artificial pupil. Using a static correction mode in the AO system, the operator corrected the natural Z_4^0 in the subject's eye before any combination of additional wavefront error was input, while the other HOAs (aside from Z_4^0) were left uncorrected. A comprehensive correction of the HOAs other than Z_4^0 may provide useful information for customized phase design without the interaction between the subject's original wavefront aberration and induced aberrations. However, this procedure will also consume more stroke of the actuators of the Mirao52 deformable mirror and limit its ability to generate a high amount of Z_6^0 (up to 0.25 µm) and combinations of Z_4^0 and Z_6^0. The subject was asked to identify the "clearest" position (centre of focus), which corresponds to the subjective best focus, and "objectionable blur" in both directions when the Badal stage was moved towards and away from the eye (representing the positive and negative direction, respectively). To measure the subjective DOF, the operator first adjusted the location of the Badal stage to allow the subject to find the "clearest" position. The scale reading of the Badal stage corresponding to the "clearest" position and the visual acuity of the subject was recorded. The operator then slowly moved the Badal stage in one direction (toward or away from the eye) which was randomly selected, until the subject noticed the appearance of "objectionable blur". The scale reading of the Badal stage was recorded by the operator. The same procedure was repeated as the operator moved the Badal stage in the opposite direction. The two recorded limits of Badal stage reading corresponding to the two locations where "objectionable blur" was observed constituted one measurement of DOF. It would have been preferable to have measured the DOF using both clear-to-blur and then blur-to-clear directions. However we compromised by using only the clear-to-blur direction to halve the testing time. Five sets of such measurements were performed for each set of Z_4^0 and Z_6^0 combination introduced to the eye. The moving speed of the Badal stage was always kept lower than 0.2 D/s. For each subject a total of 41 Z_4^0 and Z_6^0 combinations were tested. The introduction of wavefront combinations was performed in a randomized order. The whole measurement for one subject took approximately two hours to finish, including a 20-minute break after half of the wavefront combinations had been tested.

3. Results

3.1 Effect of different combinations of Z_4^0 and Z_6^0 on the DOF and visual acuity of real eyes

The individual and group mean changes in DOF of the six subjects caused by different combinations of Z_4^0 and Z_6^0 are shown in Figure 4. Increased DOF was obtained through inducing combinations of Z_4^0 and Z_6^0 to the eye. An approximately linear increase of DOF was observed with increasing levels of Z_4^0, for both positive and negative coefficients up to 0.6 μm, as shown in Figure 4a. The averaged increase in DOF was about 0.80 D for each 0.6 μm of Z_4^0 coefficient. Adding positive Z_6^0 showed slightly better efficiency in extending the DOF, with a group mean increase in DOF of 0.87 D for +0.25 μm of Z_6^0, whereas the increase in DOF was 0.70 D when -0.25 μm of Z_6^0 was added to the eyes (Figure 4b). The combination of Z_4^0 and Z_6^0 of different coefficient signs to the eye's wavefront produced some significant increases in DOF at relatively low levels of aberrations, compared with the Z_4^0 and Z_6^0 terms in isolation (Figure 4c).

Introduction of Z_4^0 and Z_6^0 also decreased the visual acuity. The group mean decrease of VA in logMAR is shown in Figure 5. Introduction of pure Z_4^0 up to 0.6 μm, either positive or negative, reduced the group mean of VA linearly at about 0.30 logMAR per μm (logMAR/μm). Inducing pure Z_6^0 up to 0.25 μm, either positive or negative, reduced the group mean of VA at about 0.83 logMAR/μm. The tested combination of Z_4^0 and Z_6^0 with different signs induced a decrease of group mean VA at about 0.40 logMAR/μm.

(Insert Figure 4 here)

(Insert Figure 5 here)

(Insert Figure 6 here)

In Figure 6, the increase of DOF has been plotted against the loss of VA caused by Z_4^0 alone, Z_6^0 alone and combinations of the two Zernike coefficients with opposite signs. Simple Z_4^0 and Z_6^0 helped to expand the DOF on average by 0.27 D and 0.24 D per 0.1 logMAR loss of VA (Pearson's correlation R^2=0.21 and R^2=0.18 respectively). However the combination of Z_4^0 and Z_6^0 was found to provide a steeper slope for DOF expansion with 0.40 D increase in DOF for every 0.1 logMAR loss of VA (Pearson's correlation R^2=0.23).

3.2 Effect of combinations of Z_4^0 and Z_6^0 on centre of focus (COF)

Introducing combinations of Z_4^0 and Z_6^0 also caused a shift of the centre of focus (COF) as determined by the subject using the Badal system adjustment. An approximately linear shift of COF was observed when Z_4^0 was induced with an average change of 2.9 D shift of centre of focus per micron of Z_4^0 (D/µm) (Figure 7a). The introduction of Z_6^0 also caused a shift of the COF by approximately –3.5 D/µm. The tested combinations of Z_4^0 and Z_6^0 of different signs caused larger shifts of COF than using Z_4^0 or Z_6^0 alone, with a shift of 3.9 D/µm of combined wavefront RMS (Figure 7c).

(Insert Figure 7 here)

4. Discussion and conclusion

The introduction of controlled levels of primary spherical aberration to the eye has been utilized clinically as a passive approach to help presbyopic patients to regain part of their near vision with multifocal contact lenses and intraocular lenses (Plakitsi & Charman, 1995; Schmidinger et al., 2006). However, the understanding of the effect on DOF of secondary spherical aberration (Z_6^0) and combinations of Z_4^0 and Z_6^0, which are naturally present in the human eye, are still limited. In this study, the ratio of increase of DOF and change of retinal image quality was used to help determine the potential optimal wavefront combinations of Z_6^0 and Z_4^0. The average DOF defined by the range of "objectionable blur" measured in six subjects was 2.59 ±0.52 D with their natural HOAs. This is a higher average value (2.59±0.52 D) compared to the value of Atchison et al (1.77 D, 2005; 1.62 D, 2009) and Legras et al (1.67D, 2010) who also used the "objectionable blur" criterion. Due to the limited number of subjects (six subjects) used in this study, it was not surprising to observe this difference in results. The requirement of subjective judgement of blur can produce significant inter-subject variance in DOF measurement. In an earlier study of Yi et al (2010), the authors reported a mean subjective DOF value of 0.79±0.15 D (ranging from 0.55 to 1.05 D) in 17 subjects, defined by the blur criterion of "just noticeable blur". A significant between-subject effect was also reported by Atchison et al (2009) on blur limits. The authors reported the most insensitive subject had a blur limit ("objectionable blur") 3.1 times larger than the most sensitive subject in their study involving seven subjects. The most insensitive subject in our study had a DOF value 1.8 times in relative to the DOF of the most sensitive subject. The magnitude of DOF defined by "objectionable blur" was found to be 2.3-2.9 times larger than the value defined by "just noticeable blur" (Atchison et al, 2005, 2009).In an earlier study, Tucker and Charman (1975) measured a DOF of a subject of approximately 2.5 D with a 6 mm pupil, using a 50% recognition criterion of 0.2 to 0.3 logMAR letter size (derived from the 6 mm curve of figure 6 of Tucker & Charman). Therefore, the mean value of 2.59±0.52 D found in this study could be regarded as at the higher end of the range of DOF defined by the "objectionable blur". Since we were measuring DOF using only a clear-to-blur direction of measurement, this may also skew the result towards a slightly higher value.

When larger amounts of Z_4^0 (up to 0.6μm) or Z_6^0 (up to 0.25μm), either positive or negative, were induced in the subject's optics, a larger DOF was generally observed. Using a similar blur criterion of "acceptable vision", Benard, Lopez-Gil and Legras (2010) reported an increase of DOF of about 1.41 dioptres per micron (D/ μm) when 0.3 and 0.6 μm of Z_4^0 were induced to the eye. In our experiment, inducing Z_4^0 or Z_6^0 alone increased, on average, the DOF by approximately 1.36 D/μm and 3.14 D/μm, respectively. When the total wavefront RMS was kept at a level less than 0.45 μm, the combined wavefront of Z_4^0 and Z_6^0 with opposite signs extended the DOF, on average, by 2.52 D/μm, compared to 3.31 D/μm reported by Benard, Lopez-Gil and Legras (2010).

Previous studies have shown that the visual system has the capacity to adapt to different levels of blur to improve discrimination (Webster et al, 2002; Elliott et al, 2011). A possible neural adaptation of the subject to their original HOAs was proposed by Artal et al (2004) and Chen et al (2007). Artal et al (2004) exposed the subjects with modified aberration patterns for up to five minutes, but did not observe any significant neural adaptation effect, while Chen et al (2007) suggested it could take up to 15 minutes. Sabesan & Yoon (2010) also suggested that the improvement in spatial vision was unlikely to be caused by temporally induced adaptation to HOAs. In present study, each induced wavefront combination was exposed to the eye for less than 3 minutes. The subject was never left to look through the static wavefront pattern for a continuous period, but was exposed to a through-focus procedure with the rate of change of defocus controlled by the experiment operator. At the end of each section of measurement, the subject was allowed to close their eyes for about 30 seconds before their pupil position was realigned for the next measurement. Therefore, the subjects should not have been exposed to any particular combination of HOA and defocus for long enough for substantial adaptation to occur.

DOF obtained under the influence of different wavefront combinations would depend on the criteria of blur adopted (Atchison et al., 2005) and spatial frequency detail of the target used (Tucker & Charman, 1975). In this study, the "objectionable blur" criterion was adopted to define the DOF. This criterion was reported to produce a DOF approximately 2.3 to 2.9 times larger than the "just noticeable blur" limits (Atchison et al., 2005, 2009). The measured DOF would also be expected to increase when a larger letter size is used for the test (Tucker & Charman, 1975; Atchison et al., 1997).

The interaction between defocus Z_2^0 and primary spherical aberration Z_4^0 was earlier investigated by Thibos et al (2002) and Applegate et al (2003b). They found that by adding Z_2^0 to Z_4^0 in the appropriate proportions, the peak-to-valley of wavefront error in the centre of the pupil can be markedly reduced, which would help to improve the retinal image quality. The authors also suggested the similar balancing between other HOAs could influence visual performance. In our experiment, we found that combinations of Z_4^0 and Z_6^0 with different signs can significantly expand the DOF, while combinations of the same sign seem to have a lower potential of improving DOF according to our numerical simulation. This finding agrees with Benard and Legras (2010), who tested 25 combinations of Z_4^0 and Z_6^0, and found the combinations more effective in extending DOF when introduced to the eye with opposite signs. This phenomenon may be explained by the interaction between the two wavefront aberrations. The Zernike polynomials describing the primary (Z_4^0) and secondary spherical aberrations (Z_6^0) are defined as

$$Z_4^0(\rho) = \sqrt{5}\,(6\rho^4 - 6\rho^2 + 1)$$

$$Z_6^0(\rho) = \sqrt{7}\,(20\rho^6 - 30\rho^4 + 12\rho^2 - 1)$$

In a wavefront combination that consists of Z_4^0 and Z_6^0 with the same sign, their common components of ρ^4 and ρ^2 compensate each other and create a flatter shape in the centre of the combined wavefront, and hence diminish the bifocal effect of the wavefront (Figure 8a). However with a combination of Z_4^0 and Z_6^0 of different signs, the multifocal feature is enhanced, as shown in Figure 8b (i.e. the peak to valley is greater).

(Insert Figure 8 here)

Using HOAs to extend the DOF also causes a trade-off between the increase of DOF and lowered VA (Piers et al., 2004; Marcos et al., 2005; Rocha et al., 2007; Rocha et al., 2009). Applegate et al (2003a) showed Z_4^0 reduced VA linearly at about 0.43 logMAR per micron (logMAR/µm) when subjects viewing a high contrast target. The authors limited the effect of subject's natural HOA by the use of a 3 mm artificial pupil and the VA measurement was achieved by viewing computer-generated aberrated images. Rouger et al (2010) reported an average loss of about 0.45 logMAR/µm of high contrast VA when subjects were tested with different levels of primary spherical aberrations through an AO visual stimulus. A much higher impact of Z_4^0 to VA of 0.81 logMAR/µm was found by Rocha et al (2007) when up to 0.9µm Z_4^0 was induced. In our experiment, introduction of pure Z_4^0 and Z_6^0 in a 6 mm pupil degraded the VA, on average, at 0.30 logMAR/µm and 0.83 logMAR/µm, respectively. While the combined wavefront of Z_4^0 and Z_6^0 reduced the VA at a rate of 0.40 logMAR/µm. The combinations of Z_4^0 and Z_6^0 of opposite signs were found to provide less impact on VA to extend the subject's DOF. For the loss of every 0.1 logMAR VA, there was an increase of 0.40 D in DOF, compared to 0.27 and 0.24 D/0.1 logMAR for Z_4^0 and Z_6^0 alone.

The shifting centre of focus (COF) under the influence of spherical aberration is important for the design of presbyopic optical corrections, since this will influence the optimal level of the spherical component of the refractive correction. A linear shift of COF averaging 2.9 dioptres per micron (D/μm) was observed when up to 0.6 μm of Z_4^0 (either positive or negative) was induced. This result was similar to that reported by Rocha et al (2009), who found an average shift of COF of 2.6 D/μm for Z_4^0, while Benard, Lopez-Gil & Legras (2010) reported a smaller value of 2.0 D/μm. The use of Z_6^0 alone shifted the COF by approximately -3.5 D/μm. The combinations of Z_4^0 and Z_6^0 of different signs produced larger shifts of COF than when either individual wavefront component was induced.

In conclusion, the results in this study show that systematic introduction of a targeted amount of both Z_4^0 and Z_6^0 can significantly improve the DOF. The use of wavefront combinations of Z_4^0 and Z_6^0 with opposite signs can further expand the DOF, than using Z_4^0 or Z_6^0 alone. It is important to determine the balance between the loss of visual quality and expanded DOF under different clinical and daily life conditions. The optimal combinations of Z_4^0 and Z_6^0 provided a better balance of DOF expansion and relatively smaller decreases in VA, which could be useful in the design of presbyopic optical corrections such as multifocal contact lenses and intraocular lenses.

Acknowledgements

We thank Prof. Larry Thibos and Prof. Richard Legras for their helpful suggestions on this manuscript.

References

Applegate, R. A., Ballentine, C., Gross, H., Sarver, E. J., & Sarver, C. A. (2003a). Visual acuity as a function of Zernike mode and level of root mean square error. *Optometry and Vision Science*, 80, 97-105.

Applegate, R. A., Marsack, J., Ramos, R., & Sarver, E. J. (2003b). Interaction between aberrations to improve or reduce visual performance. *Journal of Cataract and Refractive Surgery*, 29, 1487-1495.

Artal, P., Chen, Li., Fernández, E. J., Singer, B., Manzanera, S., & Williams, D. R. (2004). Neural compensation for the eye's optical aberrations. *Journal of Vision*, 4, 281-287.

Atchison, D. A., Charman, W. N., & Woods, R. L. (1997). Subjective depth-of-focus of the eye. *Optometry and Vision Science*, 74, 511-520.

Atchison, D. A., Collins, M. J., Wildsoet, C. F., Cristensen, J., & Waterworth, M. D. (1995). Measurement of monochromatic ocular aberrations of human eyes as a function of accommodation by the Howland aberroscope technique. *Vision Research*, 35, 313-323.

Atchison, D. A., Fisher, S. W., Pedersen, C.A., & Ridall, P. G. (2005). Noticeable, troublesome and objectionable limits of blur. *Vision Research*, 45, 1967-1974.

Benard, Y., Lopez-Gil, N., & Legras, R. (2010). Subjective depth of field in presence of 4th-order and 6th-order Zernike spherical aberrationusing adaptive optics technology. *Journal of Cataract and Refractive Surgery*, 36, 2129-2138.

Benard, Y., & Legras, R. (2010). Optimization of subjective depth of focus with combinations of spherical aberration and 6th-order spherical aberration. *Investigative Ophthalmology and Visual Science* 2010, 51: E-Abstract 3964.

Chen, L., Artal, P., Gutierrez, D., & Williams, D. R. (2007). Neural compensation for the best aberration correction. *Journal of Vision*, 7, 1-9.

Cheng, H., Barnett, J. K., Vilupuru, A. S., Marsack, J. D., Kasthurirangan, S., Applegate, R. A., & Roorda, A. (2004a). A population study on changes in wave aberrations with accommodation. *Journal of Vision*, 4, 272-280.

Cheng, X., Bradley, A., & Thibos, L. N. (2004b). Predicting subjective judgment of best focus with objective image quality metrics. *Journal of Vision*, 4, 310-321.

Collins, M. J., Franklin, R., & Davis, B. A. (2002). Optical considerations in the contact lens correction of infant aphakia. *Optometry and Vision Science*, 79, 234-240.

Elliott, S. L., Georgeson, M. A., & Webster, M. A. (2011). Response normalization and blur adaptation: Data and multi-scale model. *Journal of Vision*, 11(2):7, 1-18.

Fernández, E. J., Vabre, L., Herman, B., Unterhuber, A., Považay, B., & Drexler, W. (2006). Adaptive optics with a magnetic deformable mirror: application in the human eye. *Optics Express*, 14, 8900-8917.

He, J. C., Burns, S. A., & Marcos, S. (2000). Monochromatic aberrations in the accommodated human eye. *Vision Research*, 40, 41-48.

Iskander, D. R. (2006). Computational aspects of the visual Strehl ratio. *Optometry and Vision Science*, 83, 57-59.

Legge, G. E., Mullen, K. T., Woo, G. C., & Campbell, F. W. (1987). Tolerance to visual defocus. *Journal of Optical Society of America A*, 4, 851-863.

López-Gil, N., & Fernández-Sánchez, V. (2010). The change of spherical aberration during accommodation and its effect on the accommodation response. *Journal of Vision*, 10(13): 12, 1-15.

Manny, R. E., Fern, K. D., Zervas, H. J., Cline, G. E., Scott, S. K., White, J. M., & Pass, A. F. (1993). 1% Cyclopentolate hydrochloride: Another look at the time course of cycloplegia using an objective measure of the accommodative response. *Optometry and Vision Science*, 70, 651-665.

Marcos, S., Barbero, S., & Jimenez-Alfaro, I. (2005). Optical quality and depth-of-focus of eyes implanted with spherical and aspheric intraocular lenses. *Journal of Refractive Surgery*, 21, 223-235.

Marsack, J. D., Thibos, L. N., & Applegate, R. A. (2004). Metrics of optical quality derived from wave aberrations predict visual performance. *Journal of Vision*. 4(4):8,322-328, http://journalofvision.org/4/4/8/, doi:10.1167/4.4.8.

Neal, D. R., Baer, C. D., & Topa, D. M. (2005). Errors in Zernike transformation and non-modal reconstruction methods, *Journal of Refractive Surgery*, 21, S558-S562.

Ninomiya, S., Fujikado, T., Kuroda, T., Maeda, N., Tano, Y., Oshika, T., Hirohara, Y., & Mihashi, T. (2002). Changes of ocular aberration with accommodation. *American Journal of Ophthalmology*, 134, 924-926.

Nio, Y. K., Jansonius, N. M., Fidler, V., Geraghty, E., Norrby, S., & Kooijman, A. C. (2002). Spherical and irregular aberrations are important for the optimal performance of the human eye. *Ophthalmic and Physiological Optics*, 22, 103-112.

Piers, P. A., Fernandez, E. J., Manzanera, S., Norrby, S., & Artal, P. (2004). Adaptive optics simulation of intraocular lenses with modified spherical aberration. *Investigative Ophthalmology & Vision Science*, 45, 4601-4610.

Plakitsi, A., & Charman, W. N. (1995). Comparison of the depth of focus with the naked eye and with three types of presbyopic contact lens correction. *Journal of the British Contact Lens Association*, 18, 119-125.

Porter, J., Guirao, A., Cox, I. G., & Williams, D. R. (2001). Mono chromatic aberrations of the human eye in a large population. *Journal of the Optical Society of America A*, 18, 1793-1803.

Rocha, K. M., Soriano, E. S., Chamon, W., Chalita, M. R., & Nosé, W. (2007). Spherical aberration and depth of focus in eyes implanted with aspheric and spherical intraocular lenses. *Ophthalmology*, 114, 2050-2054.

Rocha, K. M., Vabre, L., Chateau, N., & Krueger, R. R. (2009). Expanding depth of focus by modifying higher-order aberrations induced by an adaptive optics visual simulator. *Journal of Cataract and Refractive Surgery*, 35, 1885-1892.

Rocha, K. M., Vabre, L., Harms, F., Chateau, N., & Krueger, R. R. (2007). Effects of Zernike wavefront aberrations on visual acuity measured using electromagnetic adaptive optics technology. *Journal of Refractive Surgery*, 23, 953-959.

Rouger, H., Benard, Y., & Legras, R. (2010). Effect of monochromatic induced aberrations on visual performance measured by adaptive optics technology. *Journal of Refractive Surgery*, 26, 578-587.

Sabesan, R., Ahmad, K., & Yoon, G. (2007). Correcting highly aberrated eyes using large-stroke adaptive optics. *Journal of Refractive Surgery*, 23, 947-952.

Sabesan, R., & Yoon, G. (2010) Neural compensation for long-term asymmetric optical blur to improve visual performance in keratoconic eyes. *Investigative Ophthalmology and Visual Science*, 51, 3835-3839.

Schmidinger, G., Geitzenauer, W., Hahsle, B., Klemen, U. M., Skorpik, C., & Pieh, S. (2006). Depth of focus in eyes with diffractive bifocal and refractive multifocal intraocular lenses. *Journal of Cataract and Refractive Surgery*, 32, 1650-1656.

Thibos, L. N., Hong, X., Bradley, A., & Cheng, X. (2002). Statistical variation of aberration structure and image quality in a normal population of healthy eyes. *Journal of Optical Society of America A*, 19, 2329-2348.

Tucker, J., & Charman, W. N. (1975). The depth-of-focus of the human eye for Snellen letters. American Journal of Optometry and Physiological Optics, 52, 3-21.

Wang, B., & Ciuffreda K. J. (2006) Depth-of-focus of the human eye: theory and clinical implications. *Survey of Ophthalmology*, 51, 75-85.

Wang, L., & Koch, D. D. (2003). Ocular higher-order aberrations in individuals screen for refractive surgery. *Journal of Cataract and Refractive Surgery*, 29, 1896-1903.

Webster, M. A., Georgeson, M. A., & Webster, S. M. (2002). Neural adjustment to image blur. *Nature Neuroscience*, 5, 839-840.

West, S. K., Rubin, G. S., Broman, A. T., Muñoz, B., Bandeen-Roche, K., & Turano, K. (2002). How does visual impairment affect performance on task of everyday life? The SEE Project. *Archive of Ophthalmology*, 120, 774-780.

Yi, F., Iskander, D. R., & Collins, M. J. (2010) Estimation of the depth of focus from wavefront measurements. *Journal of Vision*, 10(4)3, 1-9.

Captions to Figures

Fig. 1. (a) A flow chart of the through-focus simulation algorithm to theoretically estimate the DOF with different combinations of Z_4^0 and Z_6^0 Zernike polynomials terms. (b) An example of the output of the through-focus simulation. The modified through-focus VSOTF curve was obtained after an arbitrary level of 0.3 μm of primary spherical aberration (Z_4^0) was added to the subject's original wavefront pattern.

Fig. 2. The theoretical effect of combinations of primary and secondary spherical aberrations on the DOF of a simulated diffraction-limited model eye. (a) The effect of a total of 187 wavefront combinations has been simulated. The area of a lighter shade of grey indicates a larger increase of theoretical DOF. The boxes imposed in (a) represent the 41 wavefront combinations chosen for experimental measurement. (b) Simulated effect of pure Z_4^0 on the model eye's DOF. (c) Simulated effect of pure Z_6^0 on the model eye's DOF.

Fig. 3. Optical layout of the AO system. HASO 32 is the Hartmann Shack wavefront sensor and Mirao52 is the deformable mirror.

Fig. 4. Effect on individuals and group mean of DOF by introduction of (a) Z_4^0 alone (b) Z_6^0 alone, and (c) combinations of Z_4^0 and Z_6^0. The combined value of Z_4^0 and Z_6^0 was derived as the total RMS of the two coefficients.

Fig. 5. Decrease in VA [logMAR] of real eyes with the introduction of (a) Z_4^0 alone (b) Z_6^0 alone, and (c) combinations of Z_4^0 and Z_6^0 with opposite signs. The combined value of Z_4^0 and Z_6^0 was derived as the total RMS of the two coefficients.

Fig. 6. ΔDOF versus ΔVA induced by (a) Z_4^0 alone; (b) Z_6^0 alone; (c) combinations of Z_4^0 and Z_6^0. (d) linear fittings of all three conditions above.

Fig. 7. Shifting of COF caused by introduction of (a) Z(4,0) alone; (b) Z(6,0) alone, and (c) combinations of Z(4,0) and Z(6,0). The combined value of Z_4^0 and Z_6^0 was

derived as the total RMS of the two coefficients.

Fig. 8. (a) Wavefront combination of –0.4 µm of Z_4^0 and –0.2 µm of Z_6^0, and ; (b) Wavefront combination of –0.4 µm of Z_4^0 and 0.2 µm of Z_6^0.

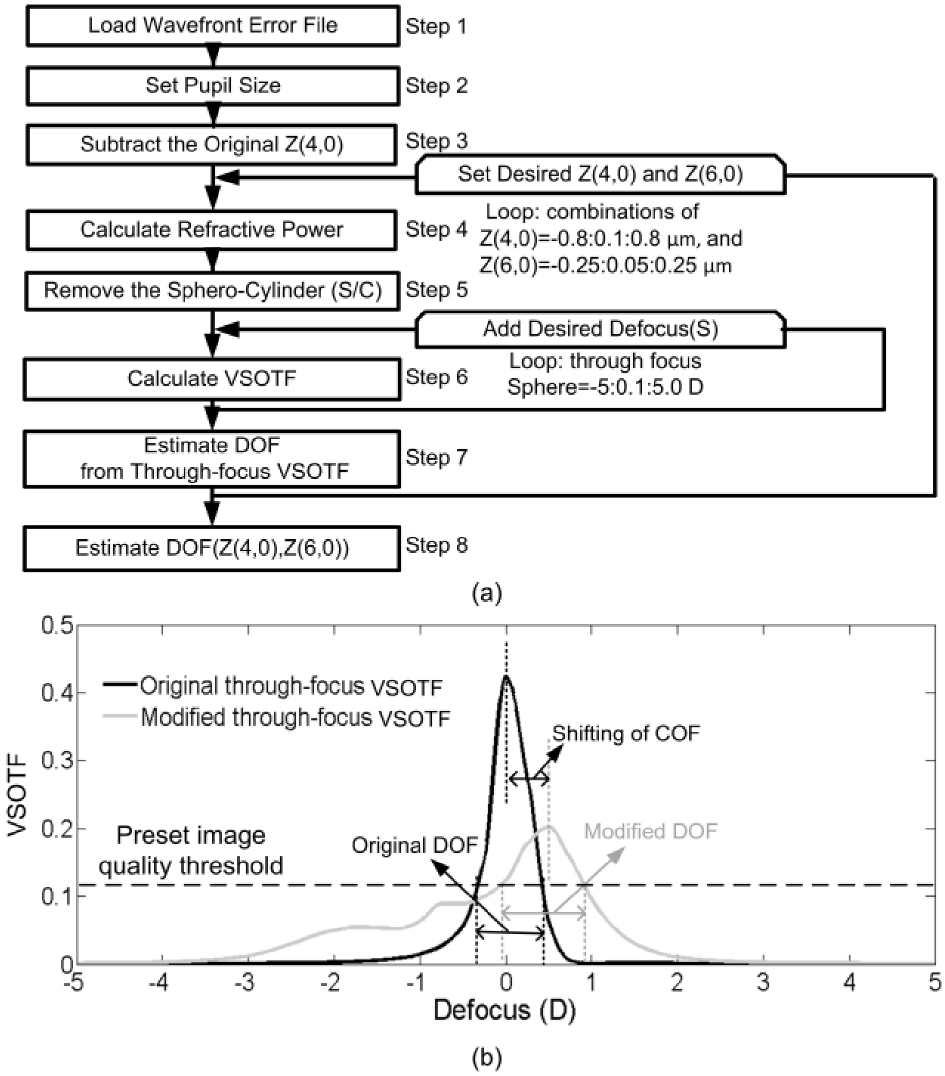
Load Wavefront Error File
Step 1
Set Pupil Size
Step 2
Subtract the Original Z(4,0)
Step 3
Set Desired Z(4,0) and Z(6,0)
Calculate Refractive Power
Step 4
Loop: combinations of
Z(4,0)=-0.8:0.1:0.8 μm, and
Z(6,0)=-0.25:0.05:0.25 μm
Remove the Sphero-Cylinder (S/C)
Step 5
Add Desired Defocus(S)
Calculate VSOTF
Step 6
Loop: through focus
Sphere=-5:0.1:5.0 D
Estimate DOF
from Through-focus VSOTF
Step 7
Estimate DOF(Z(4,0),Z(6,0))
Step 8
(a)
Original through-focus VSOTF
Modified through-focus VSOTF
Shifting of COF
VSOTF
Preset image
quality threshold
Original DOF
Modified DOF
Defocus (D)
(b)

Fig 1

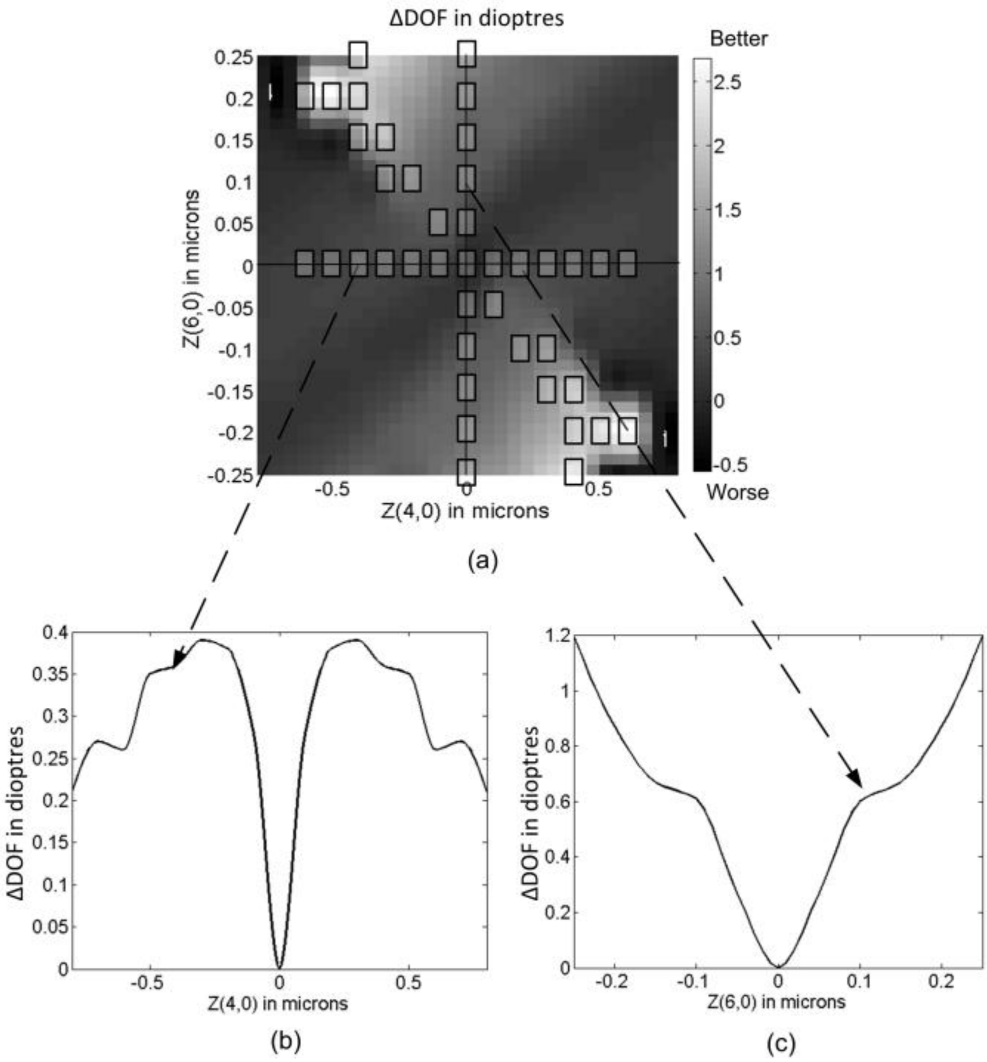

ΔDOF in dioptres
Better
Worse
Z(6,0) in microns
Z(4,0) in microns
(a)
ΔDOF in dioptres
Z(4,0) in microns
(b)
ΔDOF in dioptres
Z(6,0) in microns
(c)

Fig 2

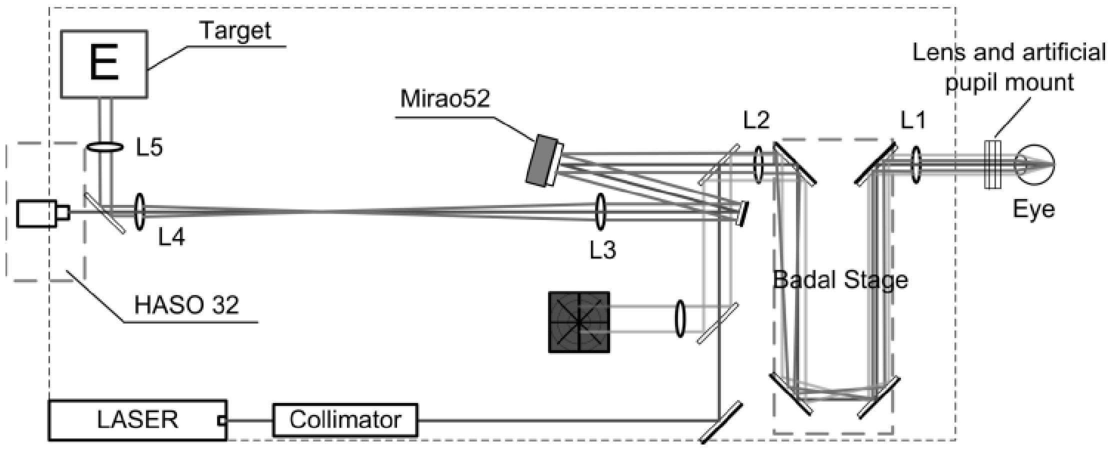
Target
E
Lens and artificial
pupil mount
Mirao52
L2
L1
L5
Eye
L4
L3
HASO 32
Badal Stage
LASER
Collimator

Fig 3

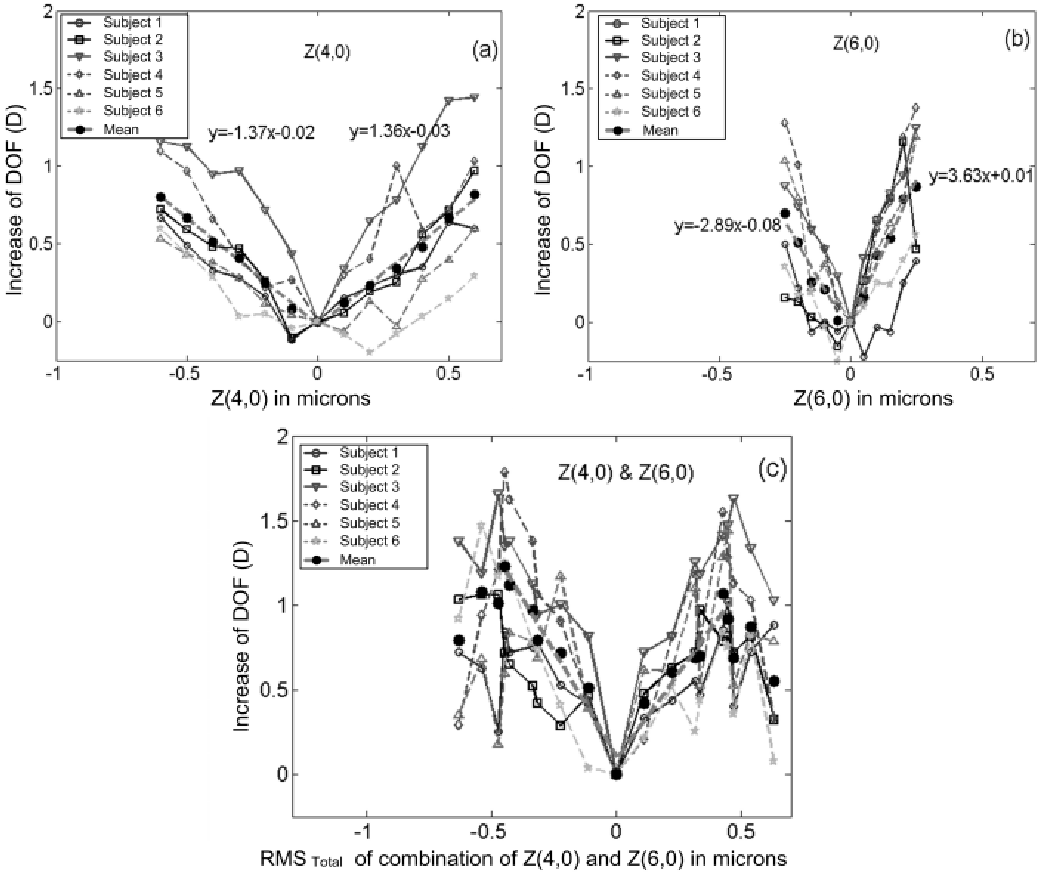
Subject 1
Subject 2
Subject 3
Subject 4
Subject 5
Subject 6
Mean
Z(4,0)
(a)
y=-1.37x-0.02
y=1.36x-0.03
Increase of DOF (D)
Z(4,0) in microns
Z(6,0)
(b)
y=-2.89x-0.08
y=3.63x+0.01
Z(6,0) in microns
Z(4,0) & Z(6,0)
(c)
RMS Total of combination of Z(4,0) and Z(6,0) in microns

Fig 4

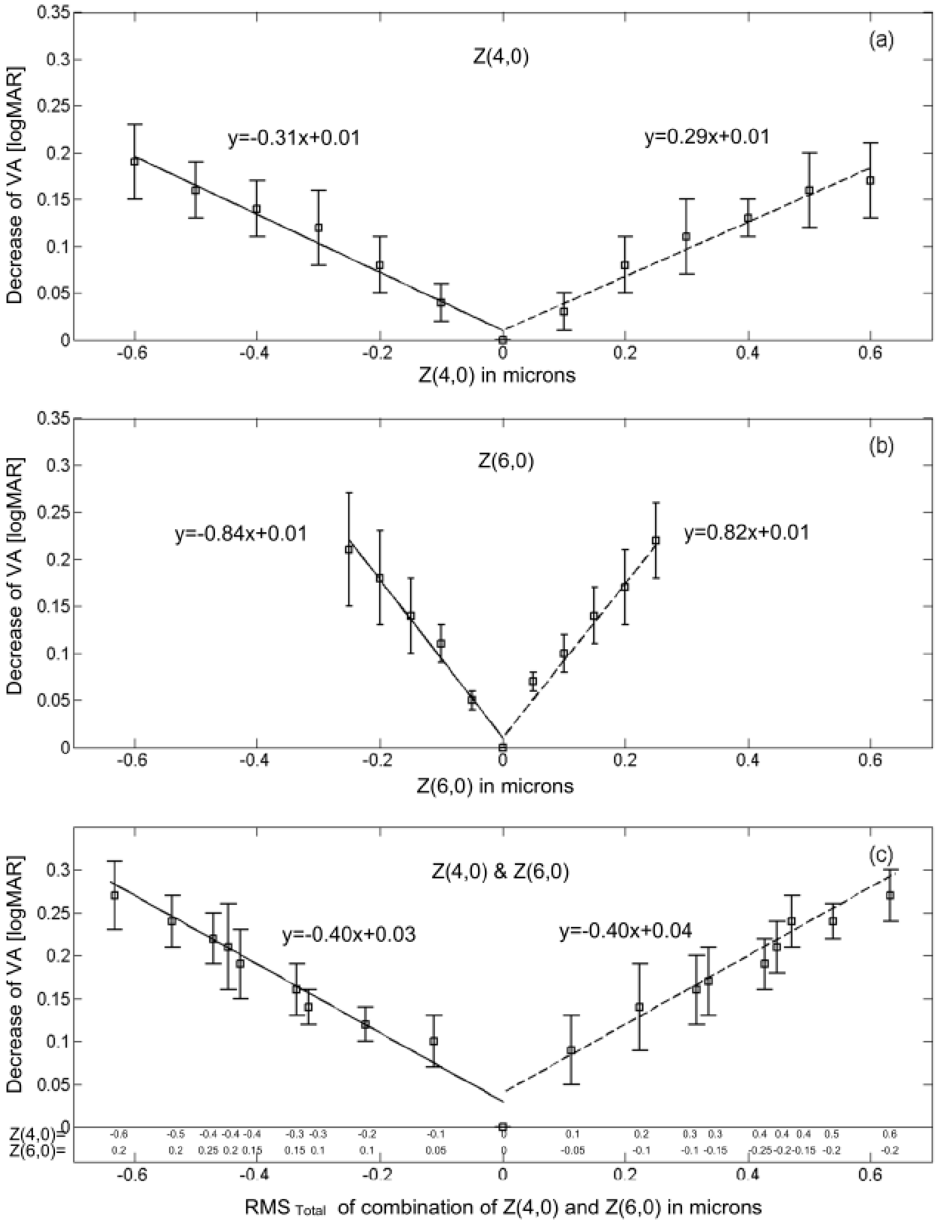
(a)
Z(4,0)
y=-0.31x+0.01
y=0.29x+0.01
Decrease of VA [logMAR]
Z(4,0) in microns
(b)
Z(6,0)
y=-0.84x+0.01
y=0.82x+0.01
Decrease of VA [logMAR]
Z(6,0) in microns
(c)
Z(4,0) & Z(6,0)
y=-0.40x+0.03
y=-0.40x+0.04
Decrease of VA [logMAR]
Z(4,0)= -0.6 -0.5 -0.4 -0.4 -0.4 -0.3 -0.3 -0.2 -0.1 0 0.1 0.2 0.3 0.3 0.4 0.4 0.4 0.5 0.6
Z(6,0)= 0.2 0.2 0.25 0.2 0.15 0.15 0.1 0.1 0.05 0 -0.05 -0.1 -0.1 -0.15 -0.25 -0.2 -0.15 -0.2 -0.2
RMS Total of combination of Z(4,0) and Z(6,0) in microns

Fig 5

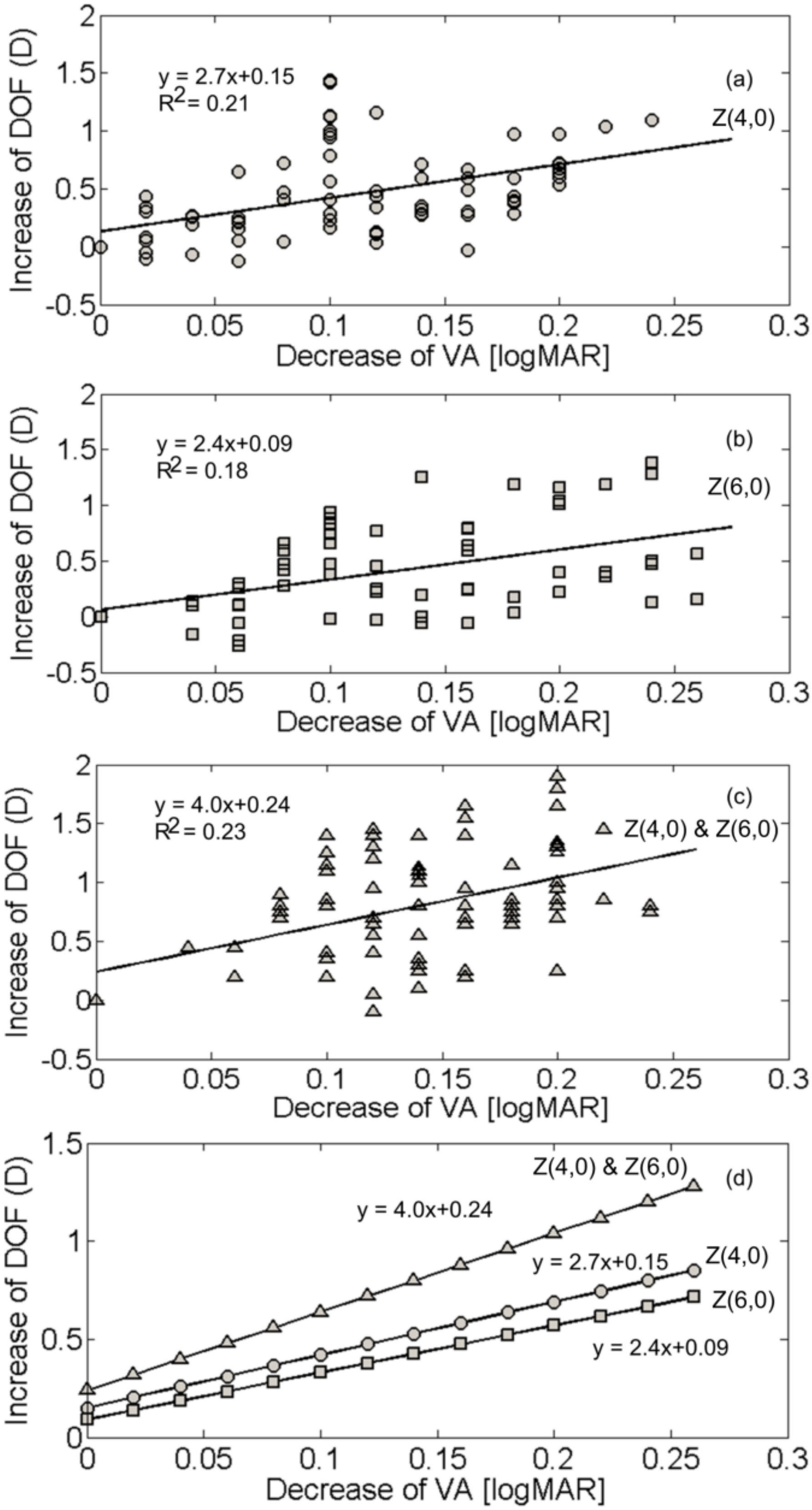
Increase of DOF (D)
y = 2.7x+0.15
R^2 = 0.21
(a)
Z(4,0)
Decrease of VA [logMAR]
Increase of DOF (D)
y = 2.4x+0.09
R^2 = 0.18
(b)
Z(6,0)
Decrease of VA [logMAR]
Increase of DOF (D)
y = 4.0x+0.24
R^2 = 0.23
(c)
Z(4,0) & Z(6,0)
Decrease of VA [logMAR]
Increase of DOF (D)
Z(4,0) & Z(6,0)
(d)
y = 4.0x+0.24
y = 2.7x+0.15
Z(4,0)
Z(6,0)
y = 2.4x+0.09
Decrease of VA [logMAR]

Fig 6

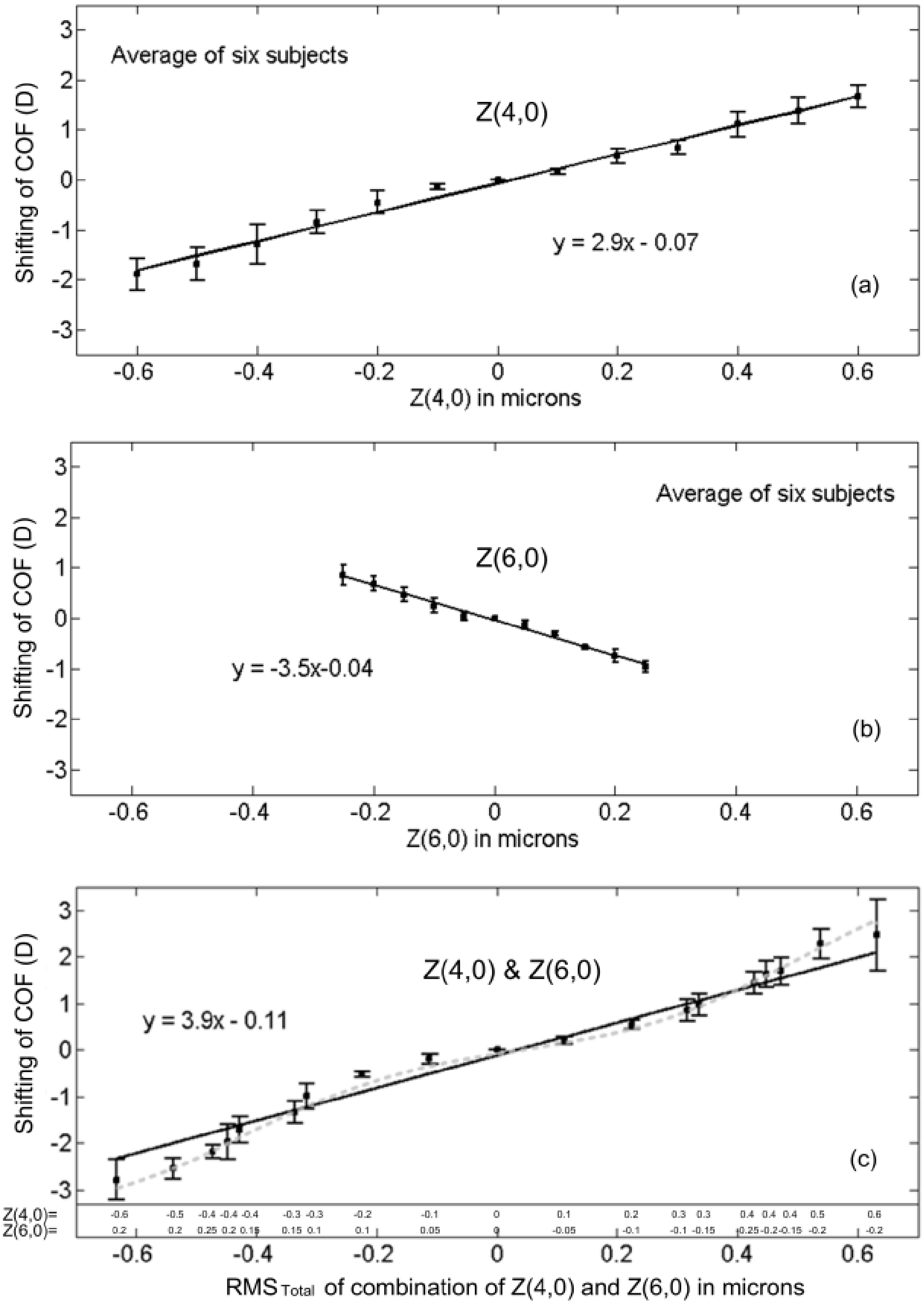
Average of six subjects
Z(4,0)
y = 2.9x - 0.07
(a)
Shifting of COF (D)
Z(4,0) in microns
Average of six subjects
Z(6,0)
y = -3.5x-0.04
(b)
Shifting of COF (D)
Z(6,0) in microns
Z(4,0) & Z(6,0)
y = 3.9x - 0.11
(c)
Shifting of COF (D)
Z(4,0)= -0.6 -0.5 -0.4 -0.4 -0.4 -0.3 -0.3 -0.2 -0.1 0 0.1 0.2 0.3 0.3 0.4 0.4 0.4 0.5 0.6
Z(6,0)= 0.2 0.2 0.25 0.2 0.15 0.15 0.1 0.1 0.05 0 -0.05 -0.1 -0.1 -0.15 -0.25 -0.2 -0.15 -0.2 -0.2
RMS Total of combination of Z(4,0) and Z(6,0) in microns

Fig 7

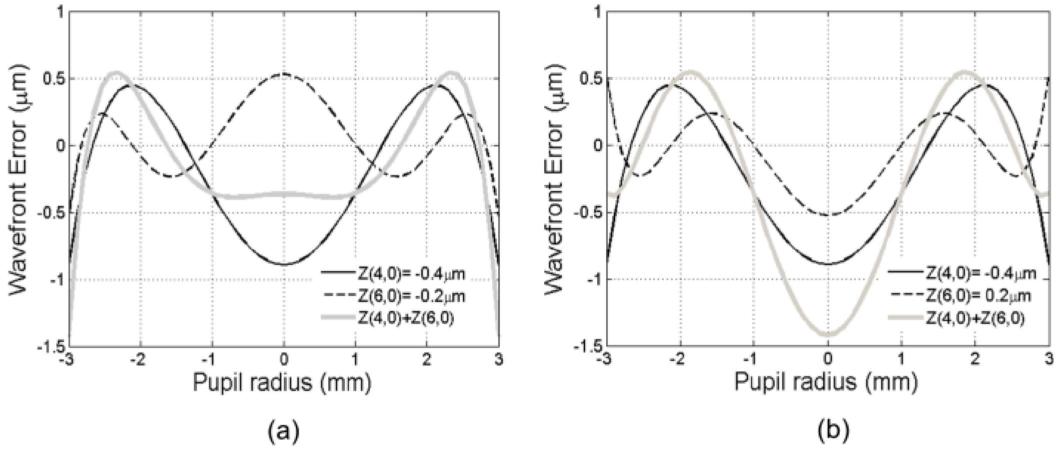

Wavefront Error (μm)
Pupil radius (mm)
Z(4,0)= -0.4μm
Z(6,0)= -0.2μm
Z(4,0)+Z(6,0)
(a)
Wavefront Error (μm)
Pupil radius (mm)
Z(4,0)= -0.4μm
Z(6,0)= 0.2μm
Z(4,0)+Z(6,0)
(b)

Fig 8